SPACE CHARGE MAP EXTRACTION AND ANALYSIS IN A DIFFERENTIAL ALGEBRAIC FRAMEWORK

A. Gee*, B. Erdelyi†
Physics Dept., Northern Illinois University, DeKalb, IL 60115, USA

Abstract

Space charge is a leading concern in high-intensity beams, causing effects such as emittance growth, beam halos, etc. As the need for high-intensity beams spreads, the demand for efficient space charge analysis grows. We developed a self consistent space charge simulation method for this purpose [1]. In order to facilitate space charge analysis, we implemented a method that allows space charge map extraction and analysis from any tracking method [1, 2]. We demonstrate the method by calculating the transverse space charge. We compare the method of moments and the fast multipole method as the tracking methods employed in the transfer map extraction process. We show results from analysis of the raw map elements as well as quantities obtained from normal forms.

INTRODUCTION

Transfer maps are powerful tools in the analysis of beam dynamics. The information even at low order is invaluable in the design and optimization of charged particle beam guidance systems. Now, we may study multi-particle beam dynamics using transfer maps. For the first time, we can extract a self-consistent space charge transfer map from simulation, opening new possibilities in the field of beam physics. Details of the theory and development can be found in [1].

The map extraction method can be employed in conjunction with any tracking method available. The map itself is smooth as it captures the mean-field limit. The tracking methods themselves are based on splitting and composition methods, more precisely Strang splitting. We implemented two tracking methods: the moment method (MoM) and the fast multipole method (FMM). The tracking methods necessarily produce slightly different results due to innate approximations, thus it is prudent to check that the map extraction procedure itself smooths out the differences, resulting in the same transfer maps for all practical purposes. That is the main goal of this paper.

A few points should be mentioned. To efficiently extract the polynomial representation of beamline elements, we employed differential algebra methods. Differential algebra methods (DA) efficiently calculate Taylor expansions to high order with machine precision and no truncation error, providing polynomial representations for any beamline element of interest. We model the space charge kick as one such element with infinitesimal length. We limit ourselves to a single space charge kick at the center of a beamline element with open boundary conditions. Furthermore, to emphasize the effects of space charge, we limited the beamline element maps to first order and calculated the space charge kick up to eighth order with the MoM and the FMM. Previous studies suggested results at the same order would be comparable.

* agee1@niu.edu
† erdelyi@anl.gov

Table 1: Beam Parameters

Species	Proton
No. of Particles	5000
Energy [MeV]	5
Shape	Ellipse
Initial spatial distribution	Uniform
Initial maximum radius [m]	0.001
Initial angle distribution	Uniform
Initial maximum angle [rad]	0.03
Initial emittance (X,Y) [μm]	(7.63 , 7.50)

BEAMLINE SIMULATION

We set up a space-charge dominant beam for our simulations. The parameters are shown in Table 1. We used the same beam conditions for all runs. We chose the number of particles, $N = 5000$, for speed with acceptable accuracy.

To analyze some simple maps, we simulated two basic examples. We set up a magnetic triplet and adjusted the quadrupole gradients to achieve imaging as our first example. Our second example is a periodic FODO cell, where we adjusted the quadrupole gradients to match an arbitrarily chosen horizontal and vertical tune.

Imaging Triplet

The triplet we set up consists of an outer drift, quad (Q1), inner drift, quad (Q2), inner drift, quad (Q3), and outer drift. The system parameters are in Table 2 and the first order system map is shown in (1).

$$\begin{pmatrix} -1 & 3.20\times10^{-14} & 0 & 0 \\ 5.69 & -1 & 0 & 0 \\ 0 & 0 & -1 & -1.91\times10^{-14} \\ 0 & 0 & -4.39 & -1 \end{pmatrix} \quad (1)$$

A ray trace of the system without space charge is also shown in Figure 1. We drew 3 independent rays in both the X-Z and Y-Z planes and generated the trajectory by applying the calculated map. The ray diagram includes an extra end drift of 6.25 cm to show the focal point at $z = 1.4$ m. This drift was left out of the system map since it would not affect our analysis.

ISBN 978-3-95450-173-1

Table 2: Imaging Triplet System Parameters

Aperture radius [m]	0.08
Outer drift lengths [m]	0.25
Inner drift lengths [m]	0.15
Q1 length [m]	0.2
Q2 length [m]	0.2
Q3 length [m]	0.2
Initial Q1 $\left[\frac{T}{m}\right]$	0.65525
Initial Q2 $\left[\frac{T}{m}\right]$	-0.66566
Initial Q3 $\left[\frac{T}{m}\right]$	0.65525

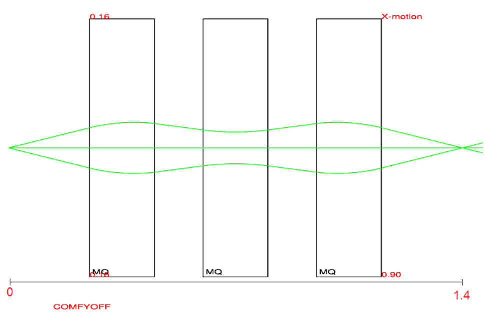

(a) X Projection

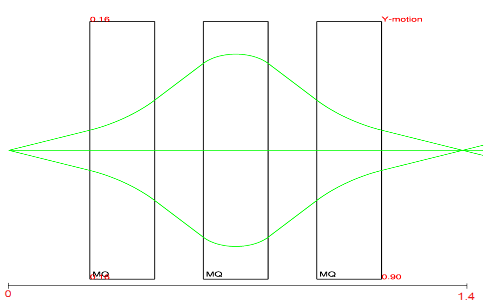

(b) Y Projection

Figure 1: Imaging triplet rays w/o space charge. Focal point is at $z = 1.4$ m.

FODO Cell

The FODO cell consists of one half quad (Q1), inner drift, full quad (Q2), inner drift, and one half quad (Q1). The system parameters are shown in Table 3. The first order system map is shown in (2). To understand its behavior, we decided to study quantities from the normal form of the map. We chose to match the system to a horizontal and vertical tune away from resonance and study its behavior.

Table 3: FODO Cell System Parameters

Aperture radius [m]	0.08
Inner drift lengths [m]	0.15
Q1 length [m]	0.1
Q2 length [m]	0.2
Initial Q1 $\left[\frac{T}{m}\right]$	-0.39045
Initial Q2 $\left[\frac{T}{m}\right]$	0.39045
Horizontal tune	0.1362
Vertical tune	0.1362

$$\begin{pmatrix} 0.656 & 0.425 & 0 & 0 \\ -1.34 & 0.656 & 0 & 0 \\ 0 & 0 & 0.656 & .951 \\ 0 & 0 & -.599 & 0.656 \end{pmatrix} \tag{2}$$

EFFECTS DUE TO SPACE CHARGE

To study the effects of space charge, we fixed the settings shown in Table 2 and Table 3. We then increased the current, or equivalently the intensity, of the beam with fixed particle number. Using the same initial beam distribution and particle quantity, the only changes must be caused by space charge for the same tracking method.

Imaging Triplet

The triplet shows some interesting behavior with higher intensity beams. From Equation 1, $(x|a)$ and $(y|b)$ are almost zero with the settings in Table 2. As the current increases, these elements grow as shown in Figure 2.

We can also see the behavior of the third order geometric aberrations $(x|x^3)$ and $(y|y^3)$ as a function of current, shown in Figure 3. Since the system map was limited to first order, the third order aberrations obtained are due to space charge. Comparing the FMM and MoM, we see the FMM predicts a slightly stronger self-field, which was seen in previous testing [3]. This is likely due inclusion of collisional forces which are negligible in the MoM. $(x|x^3)$ stands out in the beginning; space charge appears to inflate $(x|x^3)$ until around 0.25 A before reversing direction and becoming negative.

At 1.5 A, the focal point shifts as shown in Figure 4. Although subtle, the focal point is now around $z = 1.43$ m in X-Z, Figure 4a, and $z = 1.44$ m in Y-Z, Figure 4b, suggesting a slight astigmatism. The shift of the focal point is also observed due to third order terms in the system elements if included, suggesting the cause is spherical aberrations. The maximum width of the rays are increased slightly and the rays split at the point of maximum width. The split appears in both projections. This suggests a ray in Y-Z shifted in X and vice versa, leading to the extra trajectory in each projection. This split seems to come from nonlinear coupling

ISBN 978-3-95450-173-1

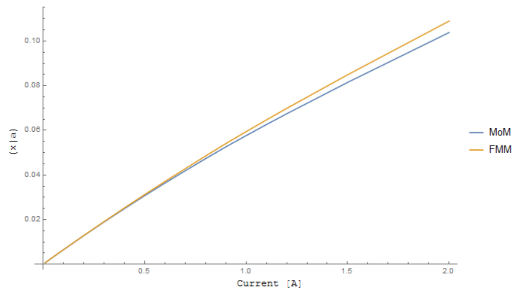

(a) $(x|a)$ vs. Current

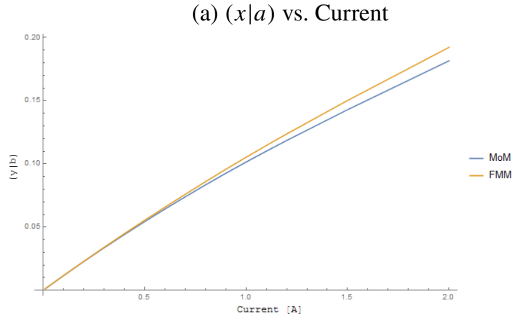

(b) $(y|b)$ vs. Current

Figure 2: Behavior of $(x|a)$ and $(y|b)$ vs. current in the imaging triplet, as calculated by the moment method and the fast multipole method.

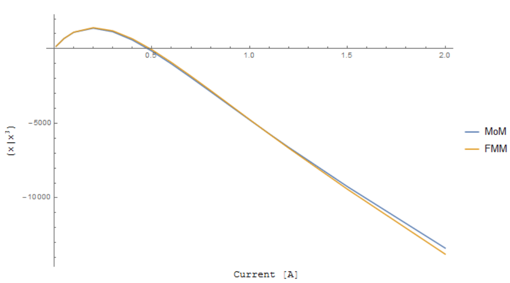

(a) $(x|x^3)$ vs. Current

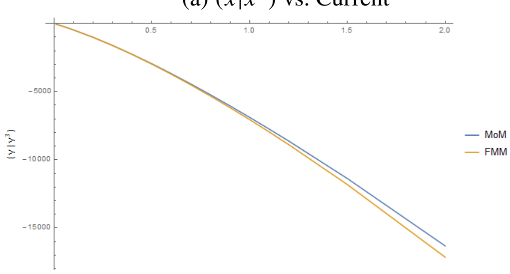

(b) $(y|y^3)$ vs. Current

Figure 3: Behavior of $(x|x^3)$ and $(y|y^3)$ vs. current in the imaging triplet, as calculated by the moment method and the fast multipole method.

introduced by fourth order space charge terms but requires more careful investigation.

FODO Cell

Settings for the quads in the FODO cell were easily found such that the calculated tunes almost perfectly matched our chosen parameters. However, its behavior changed significantly with higher intensity. From Figure 5, the deviation in the horizontal and vertical tune rapidly increases with current, displaying greater rate in the vertical. For β_x, the system stays periodic until 0.5 A, where the tune becomes imaginary. β_y's periodicity is lost around 0.3 A.

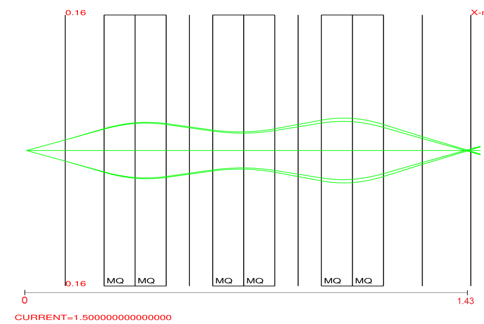

(a) X Projection

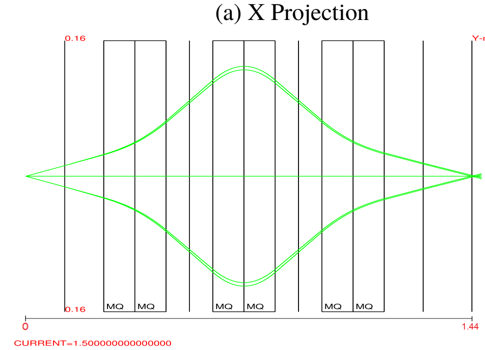

(b) Y Projection

Figure 4: Imaging Triplet rays w/ current = 1.5 A. The focal point has shifted to $z = 1.43$ m in X-Z and to $z = 1.44$ m in Y-Z.

For the FODO cell, both the MoM and FMM predict the same tune. The differences displayed in the triplet map elements suggest a very small deviation between the two methods in the map elements, which would be negligible in calculating the tune.

MINIMIZING EFFECTS DUE TO SPACE CHARGE

To reduce or eliminate the effect of space charge, we simply fit the quad gradients for each current to match our desired parameters. In some cases, the ideal solution could not be achieved, but a desired property of the system is preserved.

Imaging Triplet

In the triplet, we fit the quad gradients with the condition of only minimizing $(x|a)$ and $(y|b)$. The quad gradients steadily grew with current as shown in Figure 6. Figure 7 plots the absolute value of $(x|a)$ and $(y|b)$. These elements calculated from the FMM oddly oscillated between positive and negative values, but we are more interested in their deviation from 0. The deviation increases by about two or three orders of magnitude in $(x|a)$ and four or five orders of

ISBN 978-3-95450-173-1

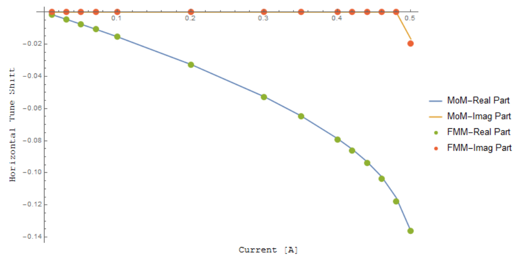

(a) Space charge induced horizontal tune shift vs. Current

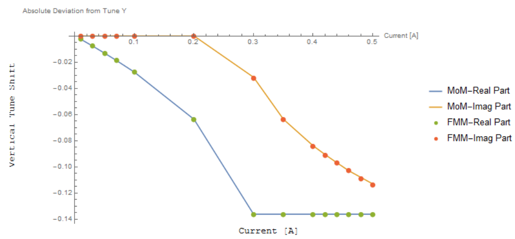

(b) Space charge induced vertical tune shift vs. Current

Figure 5: Tune shift due to space charge from tune = 0.1362 vs. current in the FODO lattice, as calculated by the moment method and the fast multipole method.

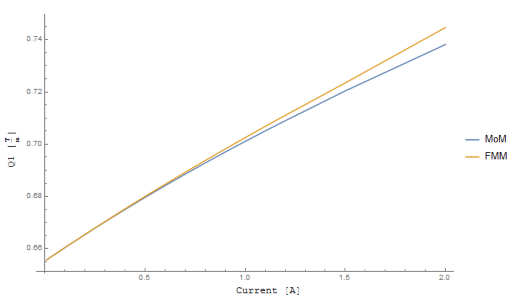

(a) Fitted Q1 vs. Current

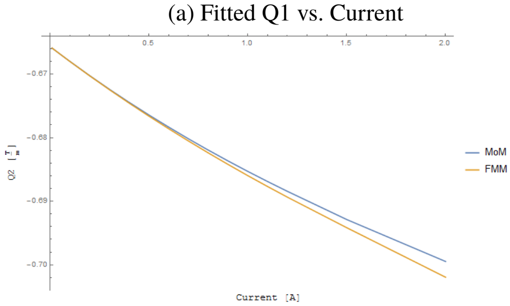

(b) Fitted Q2 vs. Current

Figure 6: Behavior of quad gradients vs. current in the imaging triplet after fitting for imaging, as calculated by the moment method and the fast multipole method.

magnitude in $(y|b)$. Again, the self-field appears stronger in Y than X, leading to the larger increase in $(y|b)$. The peak at 0.6 A in $(x|a)$ appears due to difficulty in minimizing $(x|a)$. We can also see fitting to the MoM is generally smoother than for the FMM. Most likely, this is due to the inclusion of collisional forces.

The behavior of $(x|x^3)$ and $(y|y^3)$ after fitting is shown in Figure 8. The third order aberration $(x|x^3)$ shows different behavior than before, as the two results start to diverge

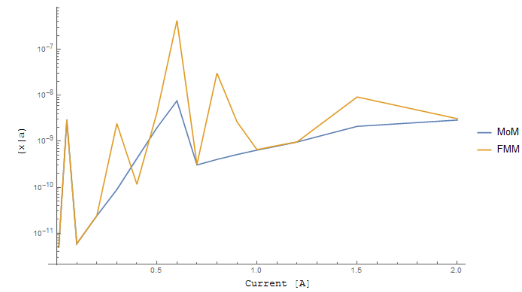

(a) $(x|a)$ vs. Current

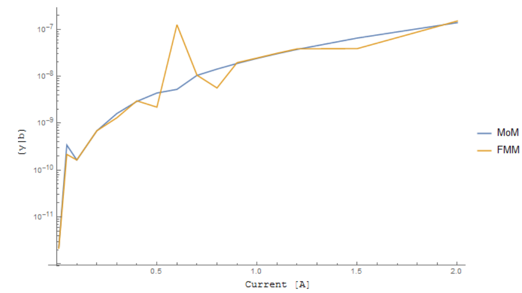

(b) $(y|b)$ vs. Current

Figure 7: Behavior of $(x|a)$ and $(y|b)$ vs. current in the imaging triplet after fitting, as calculated by the moment method and the fast multipole method.

around 0.3 A. We found this is due to the different fitted quad settings for the MoM and FMM. When using the settings found with the MoM, the FMM predicted similar $(x|x^3)$ and $(y|y^3)$ but $(x|a)$ and $(y|b)$ increased by seven orders of magnitude. This will be subject to further investigation. For $(y|y^3)$, both methods predict the aberration behaves similar to Figure 3b.

The ray diagram for 1.5 A after fitting is shown in Figure 9. Figure 9 shows the fitted quad gradients may be overcompensating as the focal points are now around $z = 1.37$ m in X-Z and $z = 1.35$ m in Y-Z. The maximum width is slightly less than in Figure 4, but the split in the ray is still present.

FODO Cell

We fit the quad gradients of the FODO Cell by matching the calculated tune to our desired tune; see Figure 10. As current increased, we found it more difficult to match the tune precisely. Vertical stability is lost around 0.3 A. To preserve stability, we allowed for higher tune fitting tolerance. Again, here the MoM and FMM give essentially identical results.

CONCLUSIONS

We presented some tests related to the performance of our self-consistent transfer map extraction method involving space charge dominated beams. The emphasis of this paper was the comparison of two different tracking methods that underlie the process, namely the Method of Moments and the Fast Multipole Method. In general, the two methods give substantially similar results. Small differences are visible at high currents due to the collisionality of the FMM versus the mean-field nature of the MoM. Still, in one case of a third

ISBN 978-3-95450-173-1

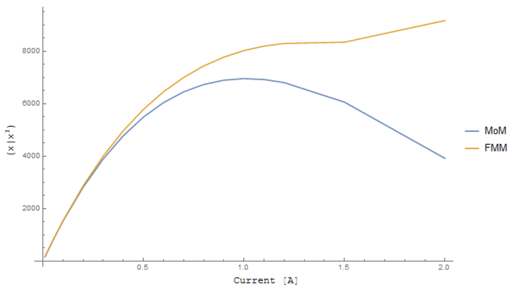

(a) $(x|x^3)$ vs. Current

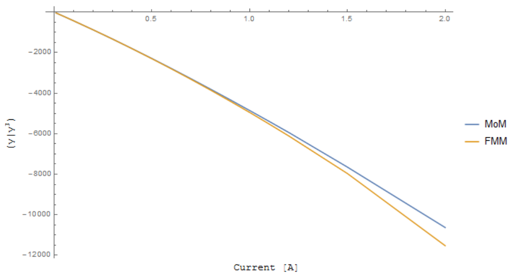

(b) $(y|y^3)$ vs. Current

Figure 8: Behavior of the geometric aberrations $(x|x^3)$ and $(y|y^3)$ vs. current in the imaging triplet after fitting, as calculated by the moment method and the fast multipole method.

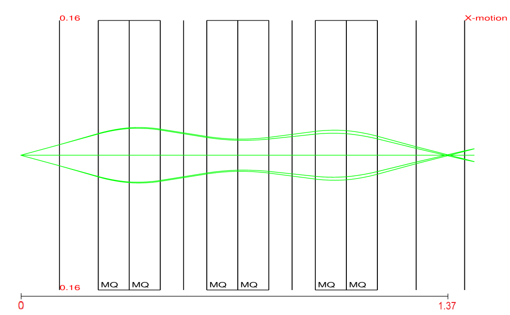

(a) X Projection

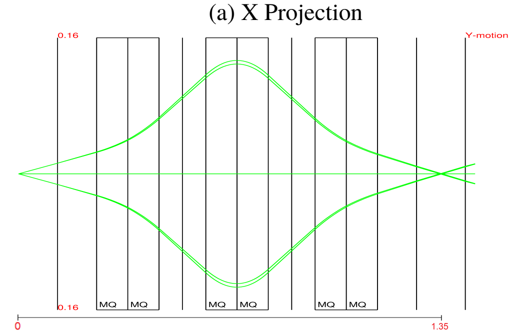

(b) Y Projection

Figure 9: Imaging Triplet rays w/ current = 1.5 A after fitting the quads for imaging. The focal points are at z = 1.37 m in X and z = 1.35 m in Y.

order spherical aberration, large discrepancy was observed due to the different settings, and this will be the subject of further studies involving larger number of particles and Plummer softening in the FMM.

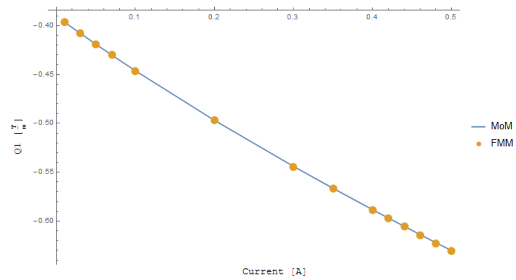

(a) Q1 vs. Current

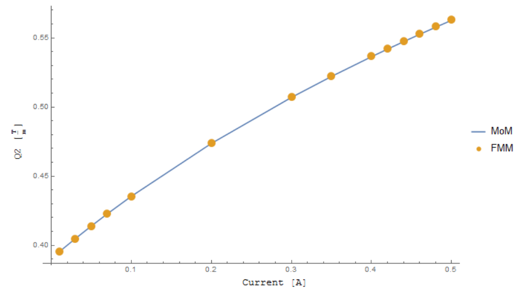

(b) Q2 vs. Current

Figure 10: Behavior of the quad gradients vs. current in the FODO lattice after fitting to the desired tune, as calculated by the moment method and the fast multipole method.

More specifically, the triplet case showed imaging properties were lost rapidly due to space charge. Spherical aberrations like $(x|x^3)$ and $(y|y^3)$ also displayed significant magnitudes. The FODO cell loses its stability quite rapidly with current, particularly in the vertical plane. When the cell is refitted, the bare tunes cannot be recovered exactly. Relaxing the constraint of equal tunes leaves more options open.

Space charge has a complex role in even these two basic examples. To control higher intensity beams, it is crucial we understand it at a fundamental level. Extracting the space charge map for analysis is a big step for beam dynamics at the intensity frontier and advancing accelerator technology.

ACKNOWLEDGMENTS

This work was supported in part by the U.S. Department of Energy, Office of High Energy Physics, under Contract Nos. DE-FG02-08ER41532 and DE-SC0011831, with Northern Illinois University.

REFERENCES

[1] B. Erdelyi, E. Nissen, and S. Manikonda, "A Differential Algebraic Method for the Solution of the Poisson Equation for Charged Particle Beams", Commun. Comput. Phys. **17**, 1, 47-78, June 2014.

[2] M. Berz, *Modern Map Methods in Particle Beam Physics*, (San Diego: Academic Press, 1999).

[3] A. Gee and B. Erdelyi, "Study and Comparison of the Method of Moments and the Single Level Fast Multipole Method for 2D Space Charge Tracking", Conf. Proc., NAPAC 2013, Pasadena, CA, USA.

ISBN 978-3-95450-173-1